Proceedings of the 7th Mediterranean Conference on Control and Automation (MED99) Haifa, Israel - June 28-30, 1999

Optimal Idle Speed Control with Induction-to-Power Finite Delay for SI Engines

Luigi Glielmo[1*] *Stefania Santini*[1†] *Gabriele Serra*[2‡]

[1]Dipartimento di Informatica e Sistemistica
Università di Napoli Federico II
via Claudio 21, 80125 Napoli, Italy

[2]Magneti Marelli Divisione Controllo Motore, Bologna, Italy

Abstract

We present an idle-speed controller designed through an optimal LQ technique taking into account during the design phase the presence of a finite time delay between variations in the manifold pressure and in the produced torque. Effectiveness of the scheme and its robustness to underestimation of the delay are shown through computer simulations.

1 Introduction

Aim of the idle speed controller for a Spark Ignition engine is to regulate the angular speed of the crankshaft in front of additional loads and disturbances, *e.g.* related to power steering or air conditioning. A number of control strategies have been proposed in the literature like PID [1], LQ [2], H_∞ [3, 4], l_1 [5], fuzzy [6], adaptive [7], sliding mode [8], neural networks [9]. The presence of a finite time delay between manifold pressure and torque generation is usually not considered in the design phase and introduces additional difficulties in the controller validation or calibration phases since it yields at least an oscillating behavior which easily degenerates into instability. Here we try to make the control design more robust in this respect and present an LQ controller designed taking explicitly into account the above-mentioned finite-delay.

2 The Structure of the Linearized Model

We consider a model of the engine obtained through linearization around the nominal conditions of engine angular speed $n = 800$ [rpm], manifold pressure $p = 300$ [mbar], spark advance $a = 20$ [degree], throttle angle $\alpha = 2.4$ [degree] (see figure 1). The model describes the dynamics in the manifold chamber, the combustion process and the crankshaft dynamics.

*Email: glielmo@disna.dis.unina.it
†PhD student supported by CNR Istituto Motori (Italian National Research Council Engine Institute). Email: santini@disna.dis.unina.it
‡Email: gabriele.serra@bologna.marelli.it

The independent variable of the differential equations is the angle of rotation of the crankshaft, to which we refer as t, measured in *Top Dead Center* (TDC) units, *i.e.* $180^{\rm o}$ of crankshaft rotation for a 4-cylinders engine. The model is detailed in the following subsections.

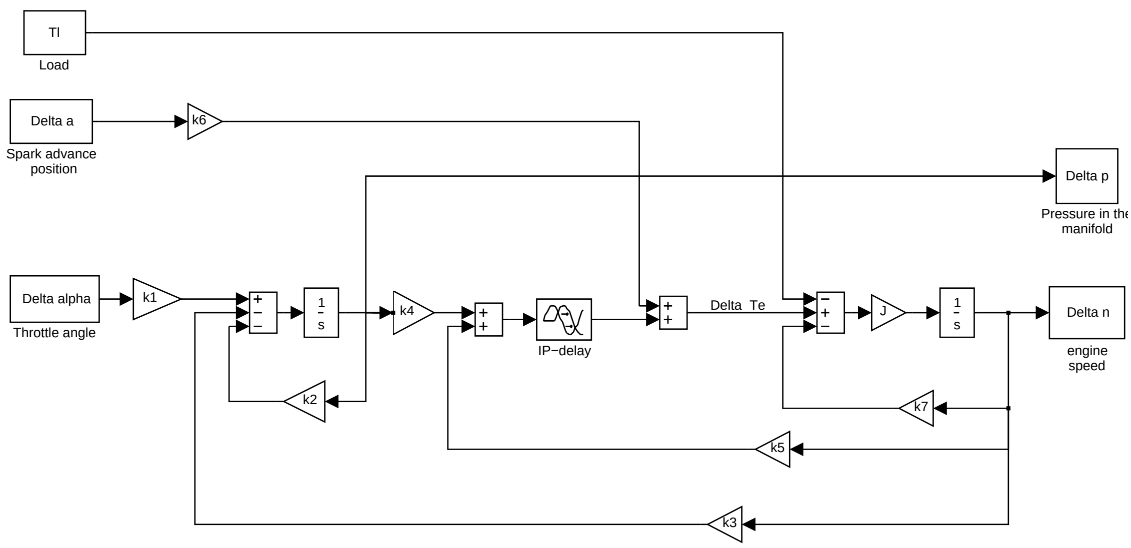

Figure 1: Simulink scheme of the system model

2.1 Dynamics in the Manifold Chamber

If the manifold chamber has no leakage, the pressure dynamics can be described by the equation [10]

$$\dot{p} = K(\dot{m}_a - \dot{m}_p), \tag{1}$$

where $\dot{m}_a$ and $\dot{m}_p$ are, respectively, the *intake* and the *engine pumping* air mass flow rate, and K depends on the volumetric capacity of the manifold, the atmospheric pressure, the air temperature, the specific heat parameters, the gas molecular weight.

Noticing that the mass flow rate $\dot{m}_a$ can be considered as a function of the throttle angle α and the manifold pressure p, and the engine pumping mass flow rate $\dot{m}_p$ is related to the manifold pressure and the angular speed n, linearization of (1) yields

$$\Delta\dot{p} = k_1\Delta\alpha - k_2\Delta p - k_3\Delta n. \tag{2}$$

2.2 Combustion Process

The combustion process is a physical phenomena with time constants much shorter than the other time constants of the engine, in particular that one of the rotational dynamics. Thus, it is possible to describe this process through algebraic relations in which its input variables (spark advance position a, manifold pressure p, engine speed n) contribute linearly to the torque production.

However the conditions in the manifold are not immediately reflected into the torque production [1]. The so called *Induction-to-Power stroke delay* $\tau_{\rm IP}$ has significant implications on control design and performance and, therefore, is explicitly considered in the model structure (see figure 1). The equation of the combustion subsystem is

$$\Delta T_e = k_4\,\Delta p(t-\tau_{\mathrm{IP}}) + k_5\,\Delta n(t-\tau_{\mathrm{IP}}) + k_6\,\Delta a, \tag{3}$$

where T_e is the torque produced.

2.3 Crankshaft Dynamics

The rotational dynamics equation is

$$J\Delta\dot{n} = \Delta T_e - T_l - k_7\,\Delta n, \tag{4}$$

where J is the moment of inertia, T_l is the external additional load torque and k_7 is the viscous friction constant.

3 The Idle Speed Control Design

The idle speed problem is formulated as a disturbance rejection problem since the main plant output (engine speed) has to be constant in spite of external disturbance torque acting on the engine crankshaft. One of the aspects to take into account is that the control action using the spark advance path is faster than using the air-channel. It turns out that a typical control action should be divided into two parts: the controller should first use the spark advance as the main control input and afterwards, as soon as the engine speed is taken care of by the air input, the spark advance should go back to its nominal value. In other words, the spark advance should exert its fast action mainly during the first part of the transient phase. To aim the control behavior in this direction the control system is structured as shown in figure 2, where one can notice that an integrator of the engine speed has been introduced to ensure zero steady-state deviation, and a derivative action

$$1 - \frac{1}{1+s\tau_d} = \frac{s\tau_d}{1+s\tau_d}$$

has been added on the spark advance signal so as to reset the advance correction soon after the intervention of the air input. A closer adherence to the real plant for the validation phase is ensured by the insertion of saturations on the input channels.

Neglecting the saturations the system is described by

$$\dot{x}(t) = A_0x(t) + A_1x(t-\tau_{\mathrm{IP}}) + Bu(t), \tag{5}$$

where $x \in \mathbb{R}^4$ and $u \in \mathbb{R}^2$ are defined in figure 2,

$$A_0 = \begin{pmatrix} -k_2 & -k_3 & 0 & 0 \\ 0 & -k_7 & -k_6/\tau_d & 0 \\ 0 & 0 & -1/\tau_d & 0 \\ 0 & 1 & 0 & 0 \end{pmatrix}, \quad A_1 = \begin{pmatrix} 0 & 0 & 0 & 0 \\ k_4 & k_5 & 0 & 0 \\ 0 & 0 & 0 & 0 \\ 0 & 0 & 0 & 0 \end{pmatrix}, \quad B = \begin{pmatrix} k_1 & 0 \\ 0 & k_6 \\ 0 & 1 \\ 0 & 0 \end{pmatrix}.$$

We introduce a quadratic performance criterion for system (5)

$$J = \int_0^\infty [x^T(t)Qx(t) + u^T(t)Ru(t)]dt, \tag{6}$$

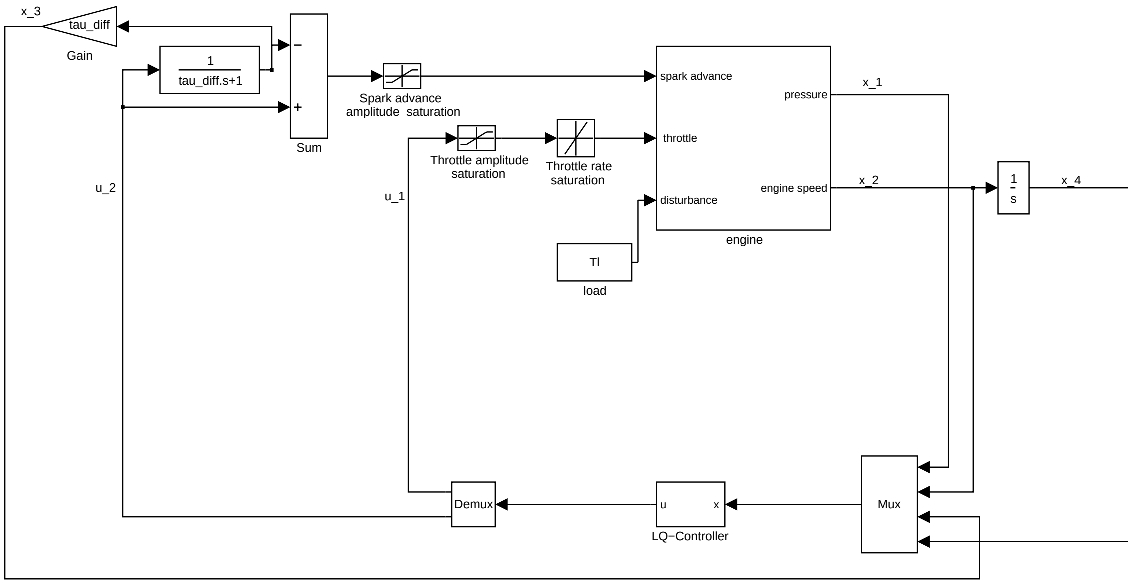

Figure 2: Closed-loop model

where Q is a symmetric positive semidefinite matrix and R is a symmetric positive definite matrix and, following [11], we assume the following structure for the feedback controller:

$$u(t) = -R^{-1}B^T K_0\, x(t) - R^{-1}B^T \int_{-\tau_{\mathrm{IP}}}^{0} K_1(\theta)\, x(t+\theta)\, d\theta. \tag{7}$$

In order to minimize the performance index the coefficients K_0, $K_1(\cdot)$ in equation (7) have to satisfy the following system of differential-algebraic equations on the rectangle $(\xi, \theta) \in [-\tau_{\mathrm{IP}}, 0]^2$ [11]:

$$\begin{aligned}
A_0^T K_0 + K_0 A_0 - K_0 B R^{-1} B^T K_0 & \\
+ {K_1}^T(0) + K_1(0) + Q &= 0, && \text{(8a)}\\
\frac{dK_1}{d\theta}(\theta) &= {A_0}^T K_1(\theta) - K_0 B R^{-1} B^T K_1(\theta) + K_2(0,\theta), && \text{(8b)}\\
\frac{\partial K_2}{\partial \xi}(\xi,\theta) + \frac{\partial K_2}{\partial \theta}(\xi,\theta) &= -{K_1}^T(\xi) B R^{-1} B^T K_1(\theta), && \text{(8c)}\\
K_1(-\tau_{\mathrm{IP}}) &= K_0 A_1, && \text{(8d)}\\
K_2(-\tau_{\mathrm{IP}}, \theta) &= A_1^T K_1(\theta). && \text{(8e)}
\end{aligned}$$

An approximate yet effective solution of (8) can be obtained by replacing equations (8b), (8c) by a finite difference scheme and requiring that equation (8e) hold at discrete times in the interval $[-\tau_{\mathrm{IP}}, 0]$. Thus, calling m a suitably chosen integer number, we form a grid of $(m+1)^2$ points on the rectangle $[-\tau_{\mathrm{IP}}, 0]^2$ with nodes $(-i\tau_{\mathrm{IP}}/m, -j\tau_{\mathrm{IP}}/m)$ for $i, j = 0, \ldots, m$. Denoting, for the sake of brevity,

$$\tilde{K}_1(i) = K_1(-i\tau_d/m) \qquad \tilde{K}_2(i,j) = K_2(-i\tau_d/m, -j\tau_d/m)$$

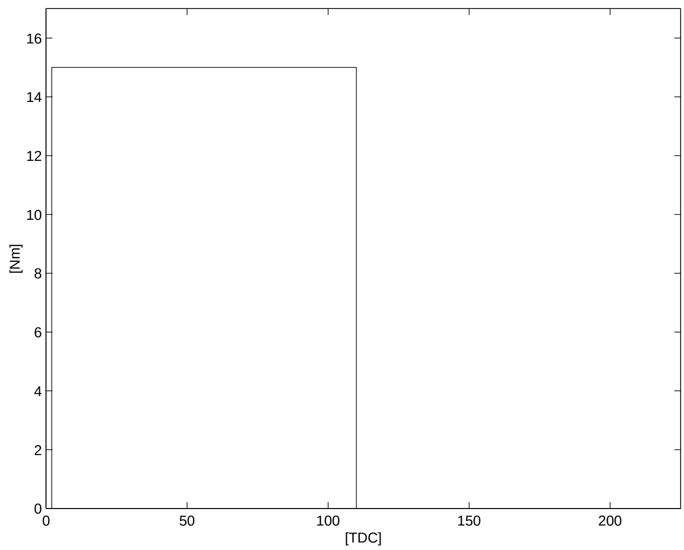

Figure 3: Disturbance torque

system (8) becomes

$$\begin{aligned}
A_0^T K_0 + K_0 A_0 - K_0 B R^{-1} B^T K_0 \qquad & \\
+ \tilde{K}_1^T(0) + \tilde{K}_1(0) + Q &= 0, && \text{(9a)}\\
[\tilde{K}_1(i-1) - \tilde{K}_1(i)]\, m/\tau_{\mathrm{IP}} &= ({A_0}^T - K_0 B R^{-1} B^T)\tilde{K}_1^T(i-1) \\
&\quad + \tilde{K}_2(0, i-1), \quad i = 1, \ldots, m, && \text{(9b)}\\
\Big\{[\tilde{K}_2(i-1, j-1) - \tilde{K}_2(i, j-1)] \qquad & \\
+ [\tilde{K}_2(i-1, j-1) - \tilde{K}_2(i-1, j)]\Big\}\, m/\tau_{\mathrm{IP}} &= -\tilde{K}_1^T(i-1) B R^{-1} B^T \tilde{K}_1(j-1) \\
&\qquad i, j = 1, \ldots, m, && \text{(9c)}\\
\tilde{K}_1(m) &= K_0 A_1, && \text{(9d)}\\
\tilde{K}_2(m, j) &= {A_1}^T \tilde{K}_1(j), \quad j = 0, \ldots, m. && \text{(9e)}
\end{aligned}$$

Once system (9) is solved, it is possible, through linear interpolation, to obtain the continuous function $K_1(\cdot)$ from the discrete function $\tilde{K}_1$.

A possible on-line implementation of the control law can be obtained sampling the state $x(t)$ with period τ_{IP}/N (with $N \geq 1$), and using linear interpolation to reconstruct the function $x(t)$ on the interval $[t - \tau_{\mathrm{IP}}, t]$ and compute the integral in (7).

4 Simulation Results

The closed loop system of figure 2 has been simulated assuming the time delay τ_{IP} to be comparable with the manifold time constant $1/k_2$ which gives, for the engine under consideration, $\tau_{\mathrm{IP}} = 5$ TDC. System (9) was solved with $m = 50$; the implementation was realized with $N = 5$. Simulation results for a disturbance load torque step of 15 Nm as of figure 3 are in figures 4, 5, 6, 7 where one can notice how the air input gradually replaces the spark advance in rejecting the disturbance.

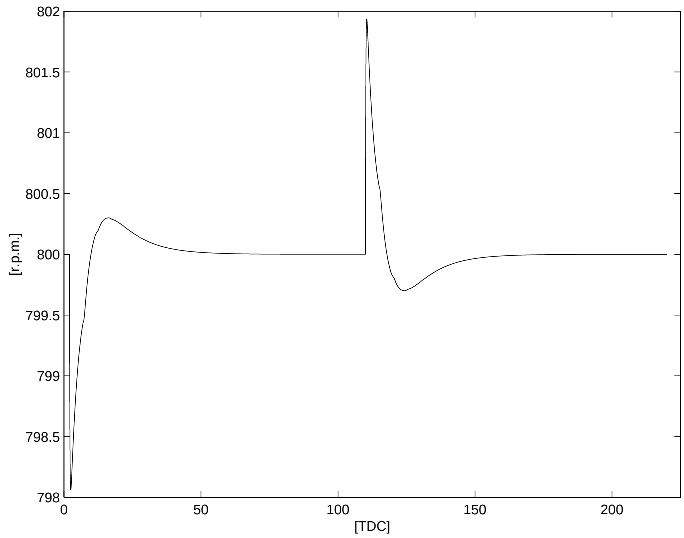

Figure 4: Engine speed

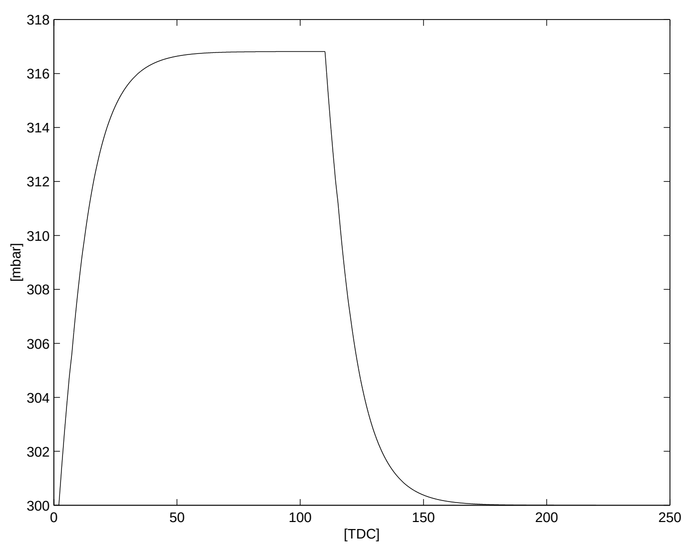

Figure 5: Pressure

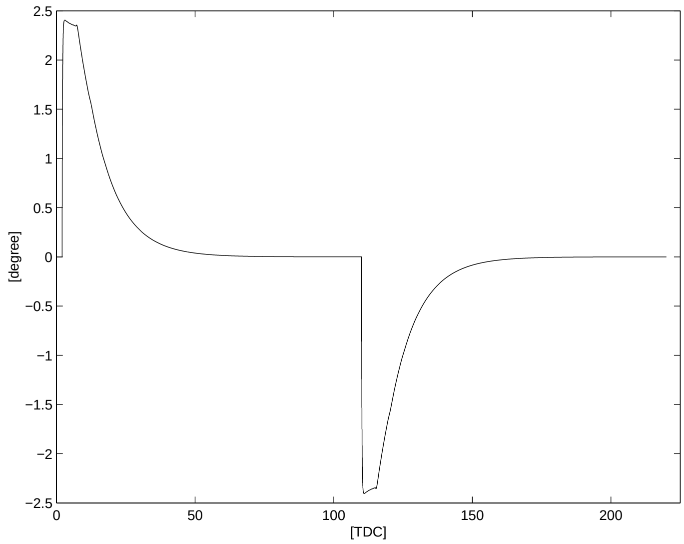

Figure 6: Variation of the spark advance w.r.t. its nominal value

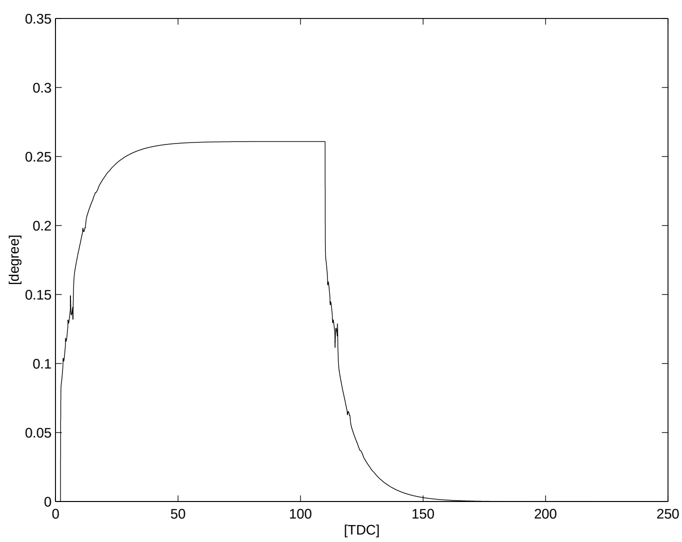

Figure 7: Variation of the throttle angle w.r.t. its nominal value

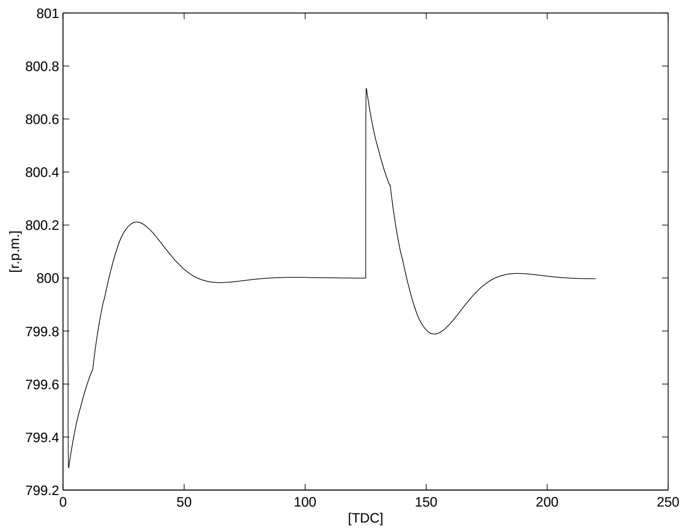

Figure 8: Engine speed ($\tau_{\mathrm{IP}} = 10$ TDC)

To test the robustness of the control scheme in front of possible variations of the finite delay duration, we employed the same controller while doubling the delay, *i.e.* $\tau_{\mathrm{IP}} = 10$ TDC. The response to the same disturbance can be found in figures 8, 9, 10, 11.

5 Conclusions

The effects of finite time delays on idle speed control are well known. Here the authors have employed an optimal control design technique which takes into account the delay and, hence, is aimed at reducing the *a posteriori* validation phase of the design. Effectiveness of the scheme and its robustness to underestimation of the delay are shown through computer simulations.

Future research will explore on one side the practical implementation of the proposed controller on a laboratory SI engine; on the other side the possibility to use the same technique to overcome the difficulties introduced by finite time delays on the spark advance input channel.

Acknowledgements

The authors wish to thank Ms. Immacolata (a.k.a. Titti) Cascella, now a fresh graduate in electronic engineering, for her contribution to this work.

References

[1] Olbrot, A. W., and B. K. Powell, ‘Robust design and analysis of third and fourth order time delay systems with application to automotive idle speed control’, *Proceedings of the American Control Conference*, 1029–1039, 1989.

[2] Morris, R. L., M. V. Warlick, and R. H. Borcherts, ‘Engine idle speed dynamics and control: a 5.81 application’, *SAE Technical Paper 820778*, 1982.

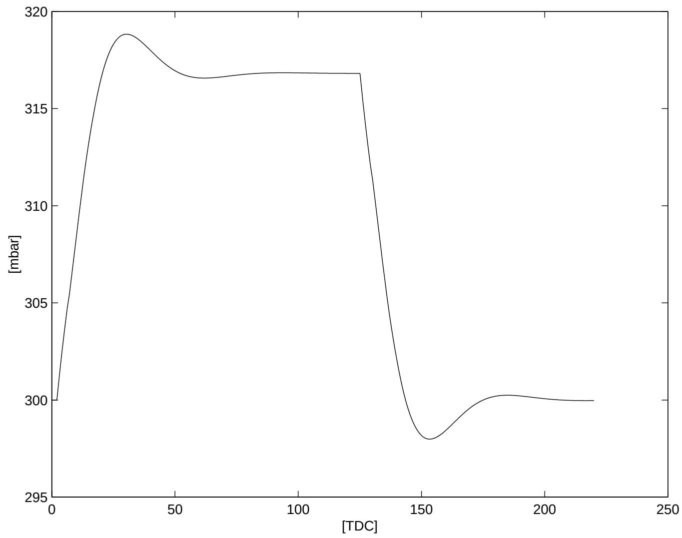

Figure 9: Pressure ($\tau_{\mathrm{IP}} = 10$ TDC)

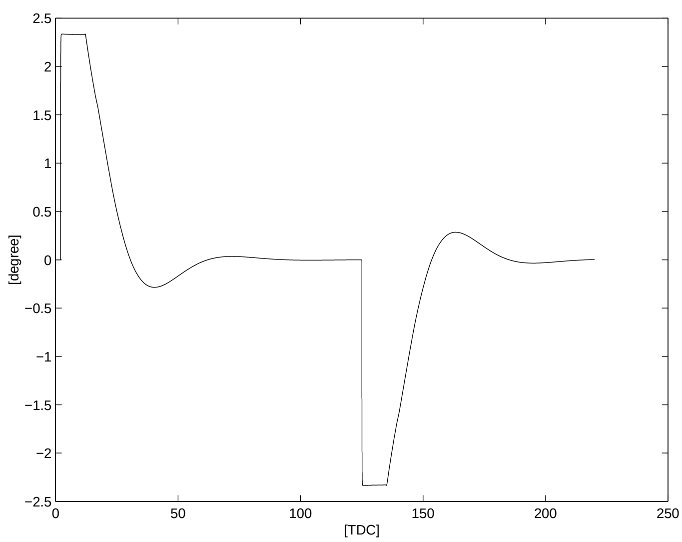

Figure 10: Variation of the spark advance w.r.t. its nominal value ($\tau_{\mathrm{IP}} = 10$ TDC)

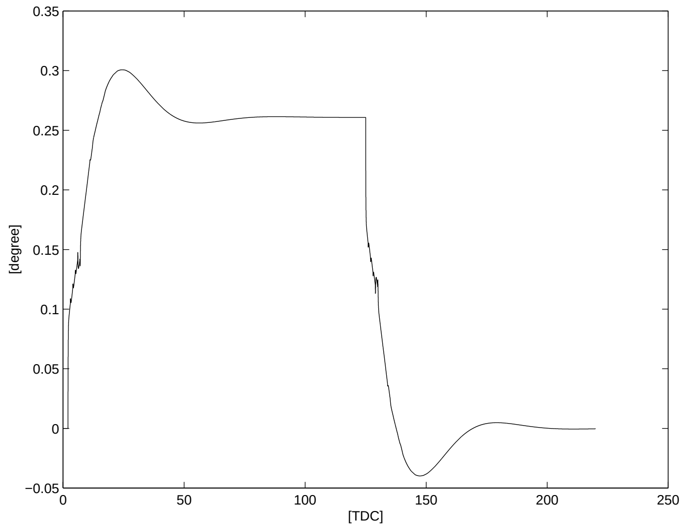

Figure 11: Variation of the throttle angle w.r.t. its nominal value ($\tau_{\rm IP} = 10$ TDC)

[3] Carnevale, C., and A. Moschetti, 'Idle speed control with H_∞ technique', *SAE Technical Paper 930770*, 1993.

[4] Williams, S. J.,D. Hrovat, C. Davey, D. Maclay, J. W. v. Crevel, and L. F. Chen, 'Idle speed control design using an H_∞ approach', *Proceedings of the American Control Conference*, 1950–1956, 1989.

[5] Butts, K., N. Sivashankar, and J. Sun, 'Feedforward and feedback design for engine idle speed control using l_1 optimization', *Proceedings of the American Control Conference*, 2587–2590, 1995.

[6] Abate, M., and N. Dosio, 'Use of fuzzy logic for engine idle speed control', *SAE Technical Paper 900594*, 1990.

[7] Osawa, M., H. Ban, and M. Myashita, 'Stochastic control for idle speed stability', *SAE Technical Paper 885066*, 1988.

[8] Kjergaard, L., S. Nielsen, T. Vesterholm, and E. Hendricks, 'Advanced nonlinear engine idle speed control system', *SAE Technical Paper 940974*, 1994.

[9] Puskorious, G. V., and L. A. Feldkamp, 'Neurocontrol of nonlinear dynamical systems with Kalman filter trained recurrent networks', *IEEE Transactions on Neural Networks*, vol. 5, no. 2, 279–297, 1994.

[10] Cook, J. A., and B. K. Powell, 'Modelling of an internal Combustion Engine for control analysis', *IEEE Control System Magazine*, 20–25, 1988.

[11] Ross, D. W., 'Controller design for time lag systems via a quadratic criterion', *IEEE Transactions on Automatic Control*, vol. AC-16, no. 6, 664–672, 1971.